Applied Numerical Mathematics 173 (2022) 193–210

Contents lists available at ScienceDirect

Applied Numerical Mathematics

www.elsevier.com/locate/apnum

Comparison of two finite element schemes for a chemo-repulsion system with quadratic production

F. Guillén-González [a,*], M.A. Rodríguez-Bellido [a], D.A. Rueda-Gómez [b]

[a] Dpto. Ecuaciones Diferenciales y Análisis Numérico and IMUS, Universidad de Sevilla, Facultad de Matemáticas, C/ Tarfia, S/N, 41012 Sevilla, Spain

[b] Escuela de Matemáticas, Universidad Industrial de Santander, A.A. 678, Bucaramanga, Colombia

ARTICLE INFO

Article history:
Received 23 July 2021
Received in revised form 15 November 2021
Accepted 2 December 2021
Available online 7 December 2021

Keywords:
Chemo-repulsion model
Quadratic production
Finite element schemes
Large-time behaviour
Energy-stability
Approximated positivity

ABSTRACT

In this paper we propose two fully discrete Finite Elements (FE) schemes for a repulsive chemotaxis model with a quadratic production term. The first one, which corresponds to the backward Euler in time with FE in space, is energy-stable in the primitive variables of the model, under a "compatibility" condition on the FE spaces. The second one, which is obtained modifying the scheme proposed in [13] by applying a regularization procedure, has an "approximated positivity" property which is obtained from discrete energy estimates and an additional estimate for a singular functional. These properties are not available in previous approaches. Additionally, we study the well-posedness and the long time behaviour of the schemes, obtaining exponential convergence to constant states as in the continuous problem. Finally, we compare the numerical schemes throughout several numerical simulations, which are in agreement with the theoretical results.

1. Introduction

The directed movement of cells in response to a chemical stimulus is known in biology as chemotaxis. More specifically, if the cells move towards regions of high chemical concentration, the motion is called chemo-attraction, while if the cells move towards regions of lower chemical concentration, the motion is called chemo-repulsion. Models for chemotaxis motion have been studied in literature (see [8,14,16–19,26,28] and references therein). One of the most important characteristics of chemoattractant models is that the blow-up of solutions can happen in space dimension greater or equal to 2; while in chemo-repulsion models this phenomenon is not expected. Many works have been devoted to study in what cases and how blow-up takes place (see for instance [4,20,25,24,27,7,30]).

In those cases in which blow-up phenomenon does not happen, it is interesting to study the asymptotic behaviour of the solutions of the model. In fact, in [23], Osaki and Yagi studied the convergence of the solution of the Keller-Segel model to a stationary solution in the one-dimensional case. In [15], the convergence of the solution of the Keller-Segel model with an additional cross-diffusion term to a steady state was shown. In [8] the authors proved the convergence to constant state for a chemo-repulsion model with linear production. Therefore, taking into account the results above, the first aim of this paper is to study the asymptotic behaviour of the following parabolic-parabolic repulsive-productive chemotaxis model (with quadratic signal production):

* Corresponding author.
E-mail addresses: guillen@us.es (F. Guillén-González), angeles@us.es (M.A. Rodríguez-Bellido), diaruego@uis.edu.co (D.A. Rueda-Gómez).

https://doi.org/10.1016/j.apnum.2021.12.001
0168-9274/

$$\begin{cases} \partial_t u - \Delta u = \nabla \cdot (u \nabla v) \ \text{ in } \Omega, \ t > 0, \\ \partial_t v - \Delta v + v = u^2 \text{ in } \ \Omega, \ t > 0, \\ \dfrac{\partial u}{\partial \mathbf{n}} = \dfrac{\partial v}{\partial \mathbf{n}} = 0 \ \text{ on } \partial\Omega, \ t > 0, \\ u(\boldsymbol{x}, 0) = u_0(\boldsymbol{x}) \geq 0, \ v(\boldsymbol{x}, 0) = v_0(\boldsymbol{x}) \geq 0 \ \text{ in } \Omega, \end{cases} \tag{1}$$

where Ω is a $n-$dimensional open bounded domain, $n = 1, 2, 3$, with boundary $\partial\Omega$; and the unknowns are $u(\boldsymbol{x}, t) \geq 0$, the cell density, and $v(\boldsymbol{x}, t) \geq 0$, the chemical concentration. This model has been studied in [12]. There, the authors showed that model (1) is well-posed: there exists global in time weak-strong solution (in the sense of Definition 2.1 below) and, for $1D$ or $2D$ domains, there exists a unique global in time regular solution.

On the other hand, another interesting topic is the study of fully discrete FE schemes approximating model (1), conserving properties of the continuous problem such as: mass-conservation, energy-stability, positivity and long time behaviour. In fact, in [13] it was studied a fully discrete FE scheme for model (1), which is mass-conservative and energy-stable with respect to a modified energy given in terms of the auxiliary variable $\boldsymbol{\sigma} = \nabla v$. However, neither energy-stability with respect to the primitive variables (u, v) (see (10) below) nor positivity (or approximated positivity) were proved. Moreover, as far as we know, there are not another works studying FE approximations for problem (1). For this reason, the second aim of this paper is to present two new fully discrete FE schemes approximating model (1), one of them is, as far as we know, the only scheme in the primitive variables (u, v) with dissipation of the exact energy; while the second scheme is the only known scheme with the property of positivity or approximated positivity for the discrete solutions.

The asymptotic behaviour of fully discrete numerical schemes has been studied in different contexts. In fact, in [10] Guillén-González and Samsidy proved asymptotic convergence for a fully discrete FE scheme for a Ginzburg-Landau model for nematic liquid crystal flow. In [21] Merlet and Pierre studied the asymptotic behaviour of the backward Euler scheme applied to gradient flows. It is important to notice that, in chemotaxis models, there are few works studying large-time behaviour for fully discrete schemes. We refer to [5], where the authors showed conditional stability and convergence at infinite time of a finite volume scheme for a Keller-Segel model with an additional cross-diffusion term. Meanwhile, the behaviour at infinite time of a fully discrete finite element scheme for model (1) seems to be still an open problem.

Likewise, the energy-stability property has been studied for fully discrete numerical schemes in the chemotaxis framework. In [11], the authors studied unconditional energy stable FE schemes for a chemo-repulsion model with linear production. A finite volume scheme for a Keller-Segel model with an additional cross-diffusion term satisfying the energy-stability property (conditionally) has been studied in [5]. In [13], it was studied an unconditionally energy-stable FE scheme for model (1) with respect to a modified energy written in terms of the auxiliary variable $\boldsymbol{\sigma} = \nabla v$. However, as we said before and up our knowledge, the energy-stability in FE schemes, with respect to the (u, v)-energy given in (10) below, is so far an open problem.

In terms of positive or approximately positive numerical schemes on chemotaxis context we refer to [6,9,31,12,11]. In [9], the nonnegativity of numerical methods, using FE techniques, to a generalized Keller-Segel model was analyzed. A discrete maximum principle for a fully discrete numerical scheme (combining the finite volume method and the nonconforming finite element method) approaching a chemotaxis-swimming bacteria model was obtained in [6]. In [11], approximated positivity of FE schemes for a chemo-repulsion model with linear production was proved. The positivity of a finite volume scheme for a parabolic-elliptic chemotaxis system was studied in [31]. In [12], positivity of only time-discrete schemes associated to model (1) was proved. However, there are not works studying positive (or approximately positive) FE schemes for model (1).

Consequently, the main novelties in this paper are the following ones:

- The introduction of a FE scheme (see scheme **UV** in Section 3 below) associated to model (1) which is energy-stable with respect to the (u, v)-energy of the continuous problem (1) given in (10), whenever a "compatibility" condition on the FE spaces holds, namely taking $(\mathbb{P}_m, \mathbb{P}_{2m})$-continuous FE (with $m \geq 1$) for (u, v).
- The introduction of another FE scheme (see scheme $\mathbf{US}_\varepsilon$ in Section 4 below) associated to model (1) which has the "approximated" positivity property for the discrete solutions. In particular, this property helps to correct the spurious oscillations around the negativity that is evidenced in other known schemes, as it can be seen in Subsections 5.1 and 5.2. The main idea lies in the obtention of first energy estimates, and then the obtention of an additional estimate for a singular functional in the variable u, which implies the approximate positivity.
- The proof of the long time behaviour for the solutions of the continuous model (1) and the discrete solutions of the schemes previously mentioned, obtaining exponential convergence to constant states as time goes to infinity.

The outline of this paper is as follows: In Section 2, we study (formally) the asymptotic behaviour of the global solutions for the model (1), and we prove the exponential convergence as time goes to infinity to constant states. In Section 3, we study a fully discrete scheme associated to model (1), corresponding to the nonlinear backward Euler in time and FE in space in the variables (u, v). The analysis includes the well-posedness of the scheme and some properties such as u-conservation, energy stability in the primitive variables (u, v), convergence towards weak solutions and long time behaviour. In Section 4, we propose another fully discrete FE approximation of model (1), which is obtained combining the scheme **US** proposed in [13] with a regularization technique. For this scheme, we can prove, in addition to the properties proved for

the previous scheme, the approximated positivity. In Section 5, we compare the numerical schemes with another numerical FE approximations throughout several numerical simulations, giving the main conclusions in Section 6.

1.1. Notation

We recall some functional spaces which will be used throughout this paper. We will consider the usual Sobolev spaces $H^m(\Omega)$ and Lebesgue spaces $L^p(\Omega)$, $1 \le p \le \infty$, with norms $\|\cdot\|_m$ and $\|\cdot\|_{L^p}$, respectively. In particular, the $L^2(\Omega)$-norm will be denoted by $\|\cdot\|_0$. We denote by $\boldsymbol{H}^1_\sigma(\Omega) := \{\mathbf{u} \in \boldsymbol{H}^1(\Omega) : \mathbf{u}\cdot\mathbf{n} = 0 \text{ on } \partial\Omega\}$ and we will use the following equivalent norms in $H^1(\Omega)$ and $\mathbf{H}^1_\sigma(\Omega)$, respectively (see [22] and [1, Corollary 3.5], respectively):

$$\|u\|_1^2 = \|\nabla u\|_0^2 + \left(\int_\Omega u\right)^2, \quad \forall u \in H^1(\Omega), \tag{2}$$

$$\|\boldsymbol{\sigma}\|_1^2 = \|\boldsymbol{\sigma}\|_0^2 + \|\mathrm{rot}\,\boldsymbol{\sigma}\|_0^2 + \|\nabla\cdot\boldsymbol{\sigma}\|_0^2, \quad \forall \boldsymbol{\sigma} \in \boldsymbol{H}^1_\sigma(\Omega). \tag{3}$$

In particular, (3) implies that

$$\|\nabla v\|_1^2 = \|\nabla v\|_0^2 + \|\Delta v\|_0^2, \quad \forall v : \nabla v \in \boldsymbol{H}^1_\sigma(\Omega).$$

If Z is a general Banach space, its topological dual will be denoted by Z'. Moreover, the letters C, C_i, K_i will denote different positive constants depending on the data (Ω, u_0, v_0), but independent of the discrete parameters (k, h) and time step n, which may change from line to line (or even within the same line).

2. Continuous problem

In this section some fundamental concepts associated to problem (1) are presented, including the definition of weak-strong solutions and some qualitative properties such as u-conservation, positivity and large time behaviour. In particular, exponential convergence to constant states as time goes to infinity is obtained.

2.1. Some properties

Problem (1) conserves in time the total mass $\int_\Omega u$. In fact, defining

$$m_0 = \frac{1}{|\Omega|}\int_\Omega u_0, \tag{4}$$

and integrating $(1)_1$ in Ω,

$$\frac{d}{dt}\left(\int_\Omega u\right) = 0, \quad \text{i.e.} \quad \int_\Omega u(t) = \int_\Omega u_0 := m_0|\Omega|, \quad \forall t > 0.$$

Now, the definition of weak-strong solutions for problem (1) is presented.

Definition 2.1. (Weak-strong solutions of (1)) Given $(u_0, v_0) \in L^2(\Omega)\times H^1(\Omega)$ with $u_0 \ge 0$, $v_0 \ge 0$ a.e. $\boldsymbol{x} \in \Omega$. A pair (u, v) is called weak-strong solution of problem (1) in $(0, +\infty)$, if $u \ge 0$, $v \ge 0$ a.e. $(t, \boldsymbol{x}) \in (0, +\infty)\times\Omega$,

$$(u - m_0, v - m_0^2) \in L^\infty(0, +\infty; L^2(\Omega)\times H^1(\Omega)) \cap L^2(0, +\infty; H^1(\Omega)\times H^2(\Omega)), \tag{5}$$

$$(\partial_t u, \partial_t v) \in L^{q'}(0, T; H^1(\Omega)'\times L^2(\Omega)), \quad \forall T > 0, \tag{6}$$

where $q' = 2$ in the 2-dimensional case $(2D)$ and $q' = 4/3$ in the 3-dimensional case $(3D)$ (q' is the conjugate exponent of $q = 2$ in $2D$ and $q = 4$ in $3D$); the following variational formulation holds

$$\int_0^T \langle \partial_t u, \overline{u}\rangle + \int_0^T (\nabla u, \nabla\overline{u}) + \int_0^T (u\nabla v, \nabla\overline{u}) = 0, \quad \forall \overline{u} \in L^q(0, T; H^1(\Omega)), \quad \forall T > 0, \tag{7}$$

the following equation pointwise holds

$$\partial_t v - \Delta v + v = u^2 \quad \text{a.e. } (t, \boldsymbol{x}) \in (0, +\infty)\times\Omega, \tag{8}$$

the initial conditions $(1)_4$ are satisfied and the following energy inequality (in integral version) holds a.e. t_0, t_1 with $t_1 \geq t_0 \geq 0$:

$$\mathcal{E}(u(t_1), v(t_1)) - \mathcal{E}(u(t_0), v(t_0)) + \int_{t_0}^{t_1} \left(\|\nabla u(s)\|_0^2 + \frac{1}{2}\|\nabla v(s)\|_1^2 \right) ds \leq 0, \tag{9}$$

where

$$\mathcal{E}(u, v) = \frac{1}{2}\|u\|_0^2 + \frac{1}{4}\|\nabla v\|_0^2. \tag{10}$$

Remark 2.2. In particular, the energy inequality (9) is valid for $t_0 = 0$. Moreover, (9) shows the dissipative character of the model with respect to the total energy $\mathcal{E}(u(t), v(t))$.

Remark 2.3. (Positivity) $u \geq 0$ in $1D$ and $2D$ domains and $v \geq 0$ in any ($1D$, $2D$ or $3D$) dimension are a consequence of (5)-(8). Indeed, this follows from the fact that in these cases we can test (7) by $u_- := \min\{u, 0\} \in L^2(0, T; H^1(\Omega))$ and (8) by $v_- := \min\{v, 0\} \in L^2(0, T; H^2(\Omega)) \hookrightarrow L^2(0, T; L^2(\Omega))$. Notice that in 3D domains, u_- has no the sufficient regularity in order to take it as test function. Hence the positivity of u cannot be deduced from (5)-(7), which must be explicitly imposed.

In [12], it was proved the existence of weak-strong solutions of problem (1) (satisfying in particular the energy inequality (9)), through convergence of a time-discrete numerical scheme associated to model (1). Hereafter, in order to abbreviate, we will use the following notation:

$$\hat{u} := u - m_0, \quad \hat{v} = v - m_0^2$$

for m_0 defined in (4).

2.2. Convergence at infinite time

In this subsection, the asymptotic analysis of problem (1) is going to be analyzed in a formal manner, without justifying the computations and assuming sufficient regularity for the exact solution (u, v). Our main interest is to reproduce the long time behaviour in fully discrete numerical schemes.

First, we define:

$$E(t) := \|\hat{u}(t)\|_0^2 + \frac{1}{2}\|\nabla v(t)\|_0^2 \text{ and } F(t) := \|\nabla \hat{u}(t)\|_0^2 + \frac{1}{2}\|\nabla v(t)\|_1^2.$$

Then, taking $\bar{u} = \hat{u}$ in (7) and testing (8) by $\bar{v} = -\frac{1}{2}\Delta v$, one arrives at (see [12] for more details)

$$\frac{1}{2}E'(t) + F(t) = 0. \tag{11}$$

Therefore, using the Poincaré inequality $\|\nabla \hat{u}\|_0^2 \geq C_p\|\hat{u}\|_0^2$ one has that $2F(t) \geq 2(C_p\|\hat{u}(t)\|_0^2 + \frac{1}{2}\|\nabla v(t)\|_1^2) \geq 2K_p E(t)$ (with $K_p = \min\{C_p, 1\}$), and from (11) one can deduce

$$E(t) \leq \|(\hat{u}_0, \nabla v_0)\|_0^2 e^{-2K_p t}, \quad \forall t \geq 0. \tag{12}$$

Moreover, testing (8) by $\bar{v} = \hat{v}$ and using (5) and (12), one has

$$\frac{d}{dt}\|\hat{v}\|_0^2 + \|\hat{v}\|_1^2 \leq C\|\hat{u}\|_0^2\|\hat{u} + 2m_0\|_{L^3}^2 \leq Ce^{-2K_p t}(1 + \|\hat{u}\|_1^2),$$

from which one arrives at

$$\|\hat{v}(t)\|_0^2 \leq \|\hat{v}_0\|_0^2 e^{-t} + Ce^{-t}\int_0^t e^{(1-2K_p)s} ds + Ce^{-t}\int_0^t e^{(1-2K_p)s}\|\hat{u}(s)\|_1^2 ds. \tag{13}$$

The last two terms on the right hand side of (13) are bounded by

$$Ce^{-t}\int_0^t e^{(1-2K_p)s} ds \leq \begin{cases} Ce^{-t} & \text{if } 2K_p > 1, \\ Cte^{-t} & \text{if } 2K_p = 1, \\ Ce^{-2K_p t} & \text{if } 2K_p < 1, \end{cases} \tag{14}$$

and

$$Ce^{-t}\int_0^t e^{(1-2K_p)s}\|\hat{u}(s)\|_1^2 ds \leq \begin{cases} Ce^{-t} & \text{if } 2K_p > 1, \\ Ce^{-t} & \text{if } 2K_p = 1, \\ Ce^{-2K_p t} & \text{if } 2K_p < 1, \end{cases} \tag{15}$$

where (5) was used in (15). Thus, from (13)-(15) one can deduce that, for any t>1,

$$\|\hat{v}(t)\|_0^2 \leq \|\hat{v}_0\|_0^2 e^{-t} + \begin{cases} Ce^{-t} & \text{if } 2K_p > 1, \\ Cte^{-t} & \text{if } 2K_p = 1, \\ Ce^{-2K_p t} & \text{if } 2K_p < 1, \end{cases} \leq C \begin{cases} e^{-t} & \text{if } 2K_p > 1, \\ te^{-t} & \text{if } 2K_p = 1, \\ e^{-2K_p t} & \text{if } 2K_p < 1. \end{cases} \tag{16}$$

3. Scheme UV

The first scheme that will be studied in this paper is obtained by using FE in space and backward Euler in time for the system (1) (considered for simplicity on a uniform partition of $[0, +\infty)$ given by $t_n = nk$, where $k > 0$ denotes the time step). Concerning the space discretization, we consider a family of shape-regular and quasi-uniform triangulations $\{\mathcal{T}_h\}_{h>0}$ of $\overline{\Omega}$ made up of simplexes (intervals in one dimension, triangles in two dimensions and tetrahedra in three dimensions), so that $\overline{\Omega} = \cup_{K\in\mathcal{T}_h} K$, where $h = \max_{K\in\mathcal{T}_h} h_K$, with h_K being the diameter of K. We choose FE spaces for u and v, which we denote by

$$(U_h, V_h) \text{ generated by } (\mathbb{P}_m, \mathbb{P}_{2m})\text{-continuous FE, with } m \geq 1.$$

With this choice, $(u_h^n)^2 \in V_h$ is guaranteed, which will be the key point to prove the energy stability of this scheme (see Lemma 3.2 below). Then, the following first order in time, nonlinear and coupled scheme is considered (hereafter, we denote $\delta_t a^n = (a^n - a^{n-1})/k$):

- *Scheme **UV**:*
  Initialization: Let $(u_h^0, v_h^0) \in U_h \times V_h$ be a suitable approximation of $(u_0, v_0) \in L^2(\Omega) \times H^1(\Omega)$, as $h \to 0$, with $\frac{1}{|\Omega|}\int_\Omega u_h^0 = \frac{1}{|\Omega|}\int_\Omega u_0 = m_0$.
  Time step n: Given $(u_h^{n-1}, v_h^{n-1}) \in U_h \times V_h$, compute $(u_h^n, v_h^n) \in U_h \times V_h$ solving

$$\begin{cases} (\delta_t u_h^n, \bar{u}_h) + (\nabla u_h^n, \nabla \bar{u}_h) + (u_h^n \nabla v_h^n, \nabla \bar{u}_h) = 0, \ \ \forall \bar{u}_h \in U_h, \\ (\delta_t v_h^n, \bar{v}_h) + (\nabla v_h^n, \nabla \bar{v}_h) + (v_h^n, \bar{v}_h) - ((u_h^n)^2, \bar{v}_h) = 0, \ \ \forall \bar{v}_h \in V_h. \end{cases} \tag{17}$$

Following similar arguments of Theorem 4.4 of [12], it can be proved unconditional solvability and conditional uniqueness of the scheme **UV**; for this reason, we will omit the details. On the other hand, for this scheme, it is not clear how to prove positivity (neither exact nor approximate) for the discrete variables u_h^n and v_h^n.

3.1. Mass-conservation, energy-stability and convergence

Since $1 \in U_h$ and $1 \in V_h$, the scheme **UV** satisfies

$$\int_\Omega u_h^n = \int_\Omega u_h^{n-1} = \cdots = \int_\Omega u_h^0 = m_0|\Omega|, \tag{18}$$

and

$$\delta_t\left(\int_\Omega v_h^n\right) = \int_\Omega (u_h^n)^2 - \int_\Omega v_h^n. \tag{19}$$

Definition 3.1. A numerical scheme with solution (u_h^n, v_h^n) is called energy-stable if the energy defined in (10) is time decreasing, that is,

$$\mathcal{E}(u_h^n, v_h^n) \leq \mathcal{E}(u_h^{n-1}, v_h^{n-1}), \ \ \forall n \geq 1.$$

Now, in order to prove the energy stability property for the scheme **UV**, we consider the linear operator $A_h : H^1(\Omega) \to V_h$ defined as follows

$$(A_h v_h, \bar{v}_h) = (\nabla v_h, \nabla \bar{v}_h) + (v_h, \bar{v}_h), \ \ \forall \bar{v}_h \in V_h. \tag{20}$$

Then, the discrete chemical equation $(17)_2$ can be rewritten as

$$(\delta_t v_h^n, \bar{v}_h) + (A_h v_h^n, \bar{v}_h) - ((u_h^n)^2, \bar{v}_h) = 0, \quad \forall \bar{v}_h \in V_h, \tag{21}$$

and the following estimate holds (see for instance, Lemma 3.1 in [13]):

$$\|v_h\|_{W^{1,6}} \leq C\|A_h v_h\|_0, \quad \forall v_h \in V_h. \tag{22}$$

Lemma 3.2. (Unconditional stability) *If (u_h^n, v_h^n) is generated by $(\mathbb{P}_m, \mathbb{P}_{2m})$-continuous FE, then the scheme **UV** is unconditionally energy-stable. In fact, if (u_h^n, v_h^n) is any solution of the scheme **UV**, then the following discrete energy law holds*

$$\delta_t \mathcal{E}(\hat{u}_h^n, v_h^n) + \frac{k}{2}\|\delta_t \hat{u}_h^n\|_0^2 + \frac{k}{4}\|\delta_t \nabla v_h^n\|_0^2 + \|\hat{u}_h^n\|_1^2 + \frac{1}{2}\|(A_h - I)v_h^n\|_0^2 + \frac{1}{2}\|\nabla v_h^n\|_0^2 = 0. \tag{23}$$

Proof. Taking $\bar{u}_h = \hat{u}_h^n$ in $(17)_1$, $\bar{v}_h = \frac{1}{2}(A_h - I)v_h^n$ in (21) and using (20), (23) is deduced. □

From the (local in time) discrete energy law (23), we deduce the following global in time estimates.

Lemma 3.3. (Uniform weak-strong estimates) *Let (u_h^n, v_h^n) be any solution of the scheme **UV**. Then, the following estimate holds*

$$\|\hat{u}_h^n\|_0^2 + \|v_h^n\|_1^2 + k\sum_{m=1}^{n}\left(\|\hat{u}_h^m\|_1^2 + \|\hat{v}_h^m\|_{W^{1,6}}^2\right) \leq C_0, \quad \forall n \geq 1, \tag{24}$$

where $W^{1,6}$ is the Sobolev space of functions in $L^6(\Omega)$ whose derivatives also belong to $L^6(\Omega)$.

Proof. Multiplying (23) by k and summing, one obtains

$$\|(\hat{u}_h^n, \nabla v_h^n)\|_0^2 + k\sum_{m=1}^{n}\left(\|\hat{u}_h^m\|_1^2 + \|\nabla v_h^m\|_0^2 + \|(A_h - I)v_h^m\|_0^2\right) \leq C_0, \quad \forall n \geq 1. \tag{25}$$

On the other hand, rewriting (17) as

$$(\delta_t \hat{v}_h^n, \bar{v}_h) + (A_h \hat{v}_h^n, \bar{v}_h) = ((\hat{u}_h^n + 2m_0)\hat{u}_h^n, \bar{v}_h), \quad \forall \bar{v}_h \in V_h, \tag{26}$$

and taking $\bar{v}_h = \hat{v}_h^n$ one has

$$\delta_t\|\hat{v}_h^n\|_0^2 + \|\hat{v}_h^n\|_1^2 \leq C\|\hat{u}_h^n + 2m_0\|_{L^{3/2}}^2\|\hat{u}_h^n\|_{L^6}^2 \leq C\|\hat{u}_h^n\|_{H^1}^2,$$

from which, multiplying by k, adding and using (25), one can deduce

$$\|v_h^n\|_0^2 + k\sum_{m=1}^{n}\|\hat{v}_h^m\|_1^2 \leq K_0, \quad \forall n \geq 1. \tag{27}$$

Then, adding (25) and (27) and using (22), (24) is obtained. □

Starting from the previous stability estimates, the convergence towards weak solutions of (1) can be proved. Concretely, by introducing the functions:

- $(\widetilde{u}_{h,k}, \widetilde{v}_{h,k})$ are continuous functions on $[0, +\infty)$, linear on each interval (t_n, t_{n+1}) and equal to (u_h^n, v_h^n) at $t = t_n$, $n \geq 0$;
- $(u_{h,k}, v_{h,k})$ are the piecewise constant functions taking values (u_h^n, v_h^n) on $(t_{n-1}, t_n]$, $n \geq 1$,

the following result holds:

Theorem 3.4. (Convergence) *There exist a subsequence (k', h') of (k, h), with $k', h' \downarrow 0$, and a weak-strong solution (u, v) of (1) in $(0, +\infty)$, such that $(\widetilde{u}_{h',k'} - m_0, \widetilde{v}_{h',k'} - m_0^2)$ and $(u_{h',k'} - m_0, v_{h',k'} - m_0^2)$ converge to $(u - m_0, v - m_0^2)$ weakly-$\star$ in $L^\infty(0, +\infty; L^2(\Omega) \times H^1(\Omega))$, weakly in $L^2(0, +\infty; H^1(\Omega) \times W^{1,6}(\Omega))$ and strongly in $L^2(0, T; L^2(\Omega) \times L^p(\Omega)) \cap C([0, T]; H^1(\Omega)' \times L^q(\Omega))$, for any $T > 0$, $1 \leq p < +\infty$ and $1 \leq q < 6$.*

Remark 3.5. Note that, since the positivity of u_h^n cannot be assured, then the positivity of the limit function u cannot be proven in the 3D case (see Remark 2.3).

Proof. Proceeding as in Theorem 4.11 of [12], one can prove that there exists a subsequence (k',h') of (k,h), with $k',h'\downarrow 0$, and (u,v) satisfying (7), (8) and the initial conditions $(1)_4$, such that $(\widetilde{u}_{h',k'}-m_0,\widetilde{v}_{h',k'}-m_0^2)$ and $(u_{h',k'}-m_0,v_{h',k'}-m_0^2)$ converge to $(u-m_0,v-m_0)$ weakly-* in $L^\infty(0,+\infty;L^2(\Omega)\times H^1(\Omega))$, weakly in $L^2(0,+\infty;H^1(\Omega)\times W^{1,6}(\Omega))$ and strongly in $L^2(0,T;L^2(\Omega)\times L^p(\Omega))\cap C([0,T];H^1(\Omega)'\times L^q(\Omega))$, for any $T>0$, $1\le p<+\infty$ and $1\le q<6$. Moreover, it holds

$$\frac{d}{dt}\left(\frac{1}{2}\|\widetilde{u}_{k',h'}(t)\|_0^2+\frac{1}{4}\|\nabla\widetilde{v}_{k',h'}(t)\|_0^2\right)+\frac{(t_n-t)}{2}\|(\delta_t u_n,\delta_t\nabla v_n)\|_0^2$$
$$+\|\nabla u_{k',h'}(t)\|_0^2+\frac{1}{2}\|(A_h-I)v_{k',h'}(t)\|_0^2+\frac{1}{2}\|\nabla v_{k',h'}(t)\|_0^2=0.$$

In order to obtain that (u,v) satisfies the energy inequality (9), it is necessary to prove that

$$\liminf_{(k',h')\to(0,0)}\int_{t_0}^{t_1}\|(A_h-I)v_{k',h'}(t)\|_0^2\ge\int_{t_0}^{t_1}\|\Delta v(t)\|_0^2. \tag{28}$$

Taking into account that $\{(A_h-I)v_{k',h'}\}$ is bounded in $L^2(0,T;L^2(\Omega))$, one has that there exists $w\in L^2(0,T;L^2(\Omega))$ such that for some subsequence of (k',h'), still denoted by (k',h'),

$$(A_h-I)v_{k',h'}\to w\quad\text{weakly in } L^2(0,T;L^2(\Omega)). \tag{29}$$

Since $u^2\in L^2(0,T;L^{3/2}(\Omega))\hookrightarrow L^2(0,T;H^1(\Omega)')$, one has

$$\partial_t v-\Delta v+v=u^2\quad\text{in } L^2(H^1)', \tag{30}$$

and, on the other hand, using (29), one can deduce

$$\partial_t v+w+v=u^2\quad\text{in } L^2(H^1)'. \tag{31}$$

Thus, from (30)-(31), one can deduce that $w=-\Delta v$ in $\mathcal{D}'(\Omega)$, and thus $-\Delta v\in L^2(0,T;L^2(\Omega))$ because of $w\in L^2(0,T;L^2(\Omega))$. Therefore, (u,v) satisfies the regularity (5) and taking into account (29), (28) is concluded. Finally, using (28) and arguing as in the last part of the proof of Theorem 4.11 of [12], it can be obtained that (u,v) satisfies the energy inequality (9), and therefore, (u,v) is a weak-strong solution of (1). □

3.2. Large-time behaviour of the scheme UV

In this subsection, exponential bounds for any solution (u_h^n,v_h^n) of the scheme **UV** in weak-strong norms are proved. The decay estimates obtained in this part (see (32) and (33) below) are a discrete version of (12) and (16).

Theorem 3.6. *Let (u_h^n,v_h^n) be a solution of the scheme **UV** associated to an initial data (u_h^0,v_h^0), with* $\frac{1}{|\Omega|}\int_\Omega u_h^0=\frac{1}{|\Omega|}\int_\Omega u_0=m_0$.

Then,

$$\|(\hat{u}_h^n,\nabla v_h^n)\|_0^2\le C_0(1+2K_pk)^{-n},\quad\forall n\ge 0, \tag{32}$$

$$\|\hat{v}_h^n\|_0^2\le\begin{cases}C(1+k)^{-n}\ \text{if } 2K_p>1,\\ C(kn)(1+k)^{-n}\ \text{if } 2K_p=1,\\ C(1+2K_pk)^{-n}\ \text{if } 2K_p<1,\end{cases} \tag{33}$$

where the constant $K_p>0$ was defined in Subsection 2.2.

Proof. Taking $\bar{u}_h=\hat{u}_h^n$ in $(17)_1$, $\bar{v}_h=\frac{1}{2}(A_h-I)v_h^n$ in (21) and using (18) and (20), one obtains

$$\delta_t\left(\frac{1}{2}\|\hat{u}_h^n\|_0^2+\frac{1}{4}\|\nabla v_h^n\|_0^2\right)+\frac{k}{2}\|\delta_t\hat{u}_h^n\|_0^2+\frac{k}{4}\|\delta_t\nabla v_h^n\|_0^2$$
$$+\|\hat{u}_h^n\|_1^2+\frac{1}{2}\|(A_h-I)v_h^n\|_0^2+\frac{1}{2}\|\nabla v_h^n\|_0^2=0. \tag{34}$$

To get (34), the fact that $(u_h^n)^2\in V_h$ is essential (which comes from the choice $(\mathbb{P}_m,\mathbb{P}_{2m})$ approximation for (U_h,V_h)) in order to cancel the terms $(u_h^n\nabla v_h^n,\nabla\hat{u}_h^n)$ and $-\frac{1}{2}((u_h^n)^2,(A_h-I)v_h^n)$. Then, from (34) one arrives at

$$(1+2K_pk)\left(\|\hat{u}_h^n\|_0^2+\frac{1}{2}\|\nabla v_h^n\|_0^2\right)-\left(\|\hat{u}_h^{n-1}\|_0^2+\frac{1}{2}\|\nabla v_h^{n-1}\|_0^2\right)\le 0,$$

from which, multiplying by $(1+2K_pk)^{n-1}$ and summing, one has for all $n \geq 0$,

$$\|\hat{u}_h^n\|_0^2 + \frac{1}{2}\|\nabla v_h^n\|_0^2 \leq (1+2K_pk)^{-n}\left(\|\hat{u}_h^0\|_0^2 + \frac{1}{2}\|\nabla v_h^0\|_0^2\right) \tag{35}$$

and (32) is obtained. On the other hand, taking $\bar{v}_h = \hat{v}_h^n$ in (26), one has

$$\frac{1}{2}\delta_t\|\hat{v}_h^n\|_0^2 + \|\hat{v}_h^n\|_1^2 \leq \int_\Omega |(\hat{u}_h^n + 2m_0)\hat{u}_h^n\hat{v}_h^n|,$$

which, using the Hölder and Young inequalities, the Sobolev embeddings $H^1(\Omega) \hookrightarrow L^6(\Omega)$ and $H^1(\Omega) \hookrightarrow L^3(\Omega)$, as well as (32), implies that

$$\begin{aligned}(1+k)\|\hat{v}_h^n\|_0^2 - \|\hat{v}_h^{n-1}\|_0^2 &\leq kC\|\hat{u}_h^n + 2m_0\|_{L^3}^2\|\hat{u}_h^n\|_0^2 \\ &\leq k\tilde{C}(1+\|\hat{u}_h^n\|_1^2)(1+2K_pk)^{-n}.\end{aligned} \tag{36}$$

Then, multiplying (36) by $(1+k)^{n-1}$ and summing, one obtains

$$(1+k)^n\|\hat{v}_h^n\|_0^2 \leq \|\hat{v}_h^0\|_0^2 + \frac{C}{1+2K_pk}k\sum_{m=1}^{n}\left(\frac{1+k}{1+2K_pk}\right)^{m-1}(1+\|\hat{u}_h^m\|_1^2). \tag{37}$$

Then, in order to obtain (33) we split the argument in three cases:

1. Case 1: If $2K_p = 1$, using (24) in (37) one has that for any $t_n = nk > 1$,

$$\|\hat{v}_h^n\|_0^2 \leq (1+k)^{-n}(C + C(kn)) \leq C(kn)(1+k)^{-n}. \tag{38}$$

2. Case 2: If $2K_p > 1$, using (24) in (37) one obtains

$$\|\hat{v}_h^n\|_0^2 \leq (1+k)^{-n}\left(C_0 + \frac{C}{2K_p - 1}\left[1 - \left(\frac{1+k}{1+2K_pk}\right)^n\right] + \frac{C}{1+2K_pk}\right) \leq C(1+k)^{-n}. \tag{39}$$

3. Case 3: If $2K_p < 1$, one rewrites (37) as

$$(1+2K_pk)^n\|\hat{v}_h^n\|_0^2 \leq \left(\frac{1+2K_pk}{1+k}\right)^n\|\hat{v}_h^0\|_0^2 + \frac{C}{1+2K_pk}k\sum_{m=1}^{n}\left(\frac{1+2K_pk}{1+k}\right)^{n-m+1}(1+\|\hat{u}_h^m\|_1^2),$$

and proceeding as in (39), taking into account that $\frac{1+2K_pk}{1+k} < 1$, one arrives at

$$\|\hat{v}_h^n\|_0^2 \leq C(1+2K_pk)^{-n}. \tag{40}$$

Therefore, from (38)-(40), (33) is deduced. □

Corollary 3.7. *Under conditions of Theorem 3.6, the following estimates hold*

$$\|(\hat{u}_h^n, \nabla v_h^n)\|_0^2 \leq C_0 e^{-\frac{2K_p}{1+2K_pk}kn}, \quad \forall n \geq 0,$$

$$\|\hat{v}_h^n\|_0^2 \leq \begin{cases} Ce^{-\frac{1}{1+k}kn} & \text{if } 2K_p > 1, \\ C(kn)e^{-\frac{1}{1+k}kn} & \text{if } 2K_p = 1, \\ Ce^{-\frac{2K_p}{1+2K_pk}kn} & \text{if } 2K_p < 1. \end{cases}$$

Proof. Using the inequality $1 - x \leq e^{-x}$ for all $x \geq 0$, from (32) one has

$$\|(\hat{u}_h^n, \nabla v_h^n)\|_0^2 \leq C_0(1+2K_pk)^{-n} \leq C_0\left(1 - \frac{2K_p}{1+2K_pk}k\right)^n \leq C_0 e^{-\frac{2K_p}{1+2K_pk}kn}. \tag{41}$$

Analogously, (33) can be deduced. □

4. Scheme $\mathbf{US}_\varepsilon$

Up to our knowledge, there are no previous works studying FE schemes for model (1), with positive or approximately positive discrete solutions. In fact, for the scheme **UV** analyzed in this paper or the scheme **US** studied in [13], it is not clear how to prove any of these properties. For this reason, in this section we propose an unconditionally energy-stable scheme with the property of "approximated positivity"; this scheme is constructed as a modification of the scheme **US** ([13]), by introducing the auxiliary variable $\boldsymbol{\sigma} = \nabla v$ and applying a regularization procedure.

4.1. Preliminary results and definition of the scheme

We consider a fully discrete approximation using FE in space and backward Euler in time for a reformulated problem in $(u, \boldsymbol{\sigma})$-variables. Moreover, in this case we will assume the following hypothesis on the space discretization:

(**H**) The triangulation is structured in the sense that all simplices have a right angle.

We choose the following continuous FE spaces for u, $\boldsymbol{\sigma}$ and v:

$$(U_h, \boldsymbol{\Sigma}_h, V_h) \subset H^1 \times \mathbf{H}^1_\sigma \times H^1 \quad \text{generated by } \mathbb{P}_1\text{-continuous FE.}$$

Remark 4.1. The right angled requirement and the choice of $\mathbb{P}_1$-continuous FE for U_h are necessary in order to obtain the relation (44) below, which is essential to define the scheme $\mathbf{US}_\varepsilon$ in (46) and to obtain its approximated positivity (see Theorem 4.10 below).

We consider the Lagrange interpolation operator $\Pi^h : C(\overline{\Omega}) \to U_h$, and we introduce the discrete semi-inner product on $C(\overline{\Omega})$ (which is an inner product in U_h) and its induced discrete seminorm (norm in U_h):

$$(u_1, u_2)^h := \int_\Omega \Pi^h(u_1 u_2), \ |u|_h = \sqrt{(u,u)^h}.$$

Remark 4.2. The norms $|\cdot|_h$ and $\|\cdot\|_0$ are equivalent in U_h, uniformly with respect to h ([3]).

We consider also the L^2-projection $Q^h : L^2(\Omega) \to U_h$ given by

$$(Q^h u, \bar{u})^h = (u, \bar{u}), \quad \forall \bar{u} \in U_h,$$

and the standard L^2-projection $\widetilde{Q}^h : L^2(\Omega) \to \boldsymbol{\Sigma}_h$. Moreover, following the ideas of Barrett and Blowey [2], we consider the truncated function $\lambda_\varepsilon : \mathbb{R} \to [\varepsilon, \varepsilon^{-1}]$ (with $\varepsilon \in (0,1)$) given by

$$\lambda_\varepsilon(s) := \begin{cases} \varepsilon & \text{if} \quad s \le \varepsilon, \\ s & \text{if} \quad \varepsilon \le s \le \varepsilon^{-1}, \\ \varepsilon^{-1} & \text{if} \quad s \ge \varepsilon^{-1}. \end{cases}$$

If we define

$$F''_\varepsilon(s) := \frac{1}{\lambda_\varepsilon(s)}, \tag{42}$$

then, we can integrate twice in (42), imposing the conditions $F'_\varepsilon(1) = F_\varepsilon(1) = 0$, and we obtain a convex function $F_\varepsilon : \mathbb{R} \to [0, +\infty)$, such that $F_\varepsilon \in C^2(\mathbb{R})$. Even more, for $\varepsilon \in (0, e^{-2})$, it holds (see [2])

$$F_\varepsilon(s) \ge \frac{\varepsilon}{2} s^2 - 2 \ \ \forall s \ge 0 \quad \text{and} \quad F_\varepsilon(s) \ge \frac{s^2}{2\varepsilon} \ \ \forall s \le 0. \tag{43}$$

Then, for each $\varepsilon \in (0,1)$ we consider the construction of the operator $\Lambda_\varepsilon : U_h \to L^\infty(\Omega)^{d\times d}$ given in [2], satisfying that $\Lambda_\varepsilon u^h$ is a piecewise constant matrix for all $u^h \in U_h$, such that the following relation holds

$$(\Lambda_\varepsilon u^h) \nabla \Pi^h(F'_\varepsilon(u^h)) = \nabla u^h \quad \text{in } \Omega. \tag{44}$$

Basically, $\Lambda_\varepsilon u^h$ is a constant by elements symmetric and positive definite matrix such that (44) holds by elements. We highlight that (44) is satisfied due to the right angled constraint requirement (**H**) and the choice of $\mathbb{P}_1$-continuous FE for U_h. We recall the result below concerning to $\Lambda_\varepsilon(\cdot)$ (see [2, Lemma 2.1]).

Lemma 4.3. *Let $\|\cdot\|$ denote the spectral norm on $\mathbb{R}^{d\times d}$. Then for any given $\varepsilon\in(0,1)$ the function $\Lambda_\varepsilon : U_h \to [L^\infty(\Omega)]^{d\times d}$ is continuous and satisfies*

$$\varepsilon\xi^T\xi \le \xi^T\Lambda_\varepsilon(u^h)\xi \le \varepsilon^{-1}\xi^T\xi,\ \ \forall\xi\in\mathbb{R}^d,\ \forall u^h\in U_h. \tag{45}$$

Then, the following first order in time, nonlinear and coupled scheme is considered:

- *Scheme* $\mathbf{US}_\varepsilon$:
  Initialization: Let $(u_h^0,\boldsymbol{\sigma}_h^0,v_h^0)=(Q^hu_0,\widetilde{Q}^h(\nabla v_0),Q^hv_0)\in U_h\times\boldsymbol{\Sigma}_h\times V_h$. In particular, $\frac{1}{|\Omega|}\int_\Omega u_h^0=\frac{1}{|\Omega|}\int_\Omega u_0=m_0$, $u_h^0\ge 0$ and $v_h^0\ge 0$.
  Time step n: Given $(u_\varepsilon^{n-1},\boldsymbol{\sigma}_\varepsilon^{n-1})\in U_h\times\boldsymbol{\Sigma}_h$, compute $(u_\varepsilon^n,\boldsymbol{\sigma}_\varepsilon^n)\in U_h\times\boldsymbol{\Sigma}_h$ solving

$$\begin{cases}(\delta_t u_\varepsilon^n,\bar u)^h+(\nabla u_\varepsilon^n,\nabla\bar u)+(\Lambda_\varepsilon(u_\varepsilon^n)\boldsymbol{\sigma}_\varepsilon^n,\nabla\bar u)=0,\ \ \forall\bar u\in U_h,\\ (\delta_t\boldsymbol{\sigma}_\varepsilon^n,\bar{\boldsymbol{\sigma}})+(B_h\boldsymbol{\sigma}_\varepsilon^n,\bar{\boldsymbol{\sigma}})=2(\Lambda_\varepsilon(u_\varepsilon^n)\nabla u_\varepsilon^n,\bar{\boldsymbol{\sigma}}),\ \ \forall\bar{\boldsymbol{\sigma}}\in\Sigma_h,\end{cases} \tag{46}$$

  where the linear operator $B_h:\boldsymbol{\Sigma}_h\to\boldsymbol{\Sigma}_h$ is defined as

$$(B_h\boldsymbol{\sigma}_\varepsilon^n,\bar{\boldsymbol{\sigma}})=(\nabla\cdot\boldsymbol{\sigma}_\varepsilon^n,\nabla\cdot\bar{\boldsymbol{\sigma}})+(\mathrm{rot}\,\boldsymbol{\sigma}_\varepsilon^n,\mathrm{rot}\,\bar{\boldsymbol{\sigma}})+(\boldsymbol{\sigma}_\varepsilon^n,\bar{\boldsymbol{\sigma}}),\ \ \forall\bar{\boldsymbol{\sigma}}\in\boldsymbol{\Sigma}_h.$$

Once the scheme $\mathbf{US}_\varepsilon$ is solved, given $v_\varepsilon^{n-1}\in V_h$, we can recover $v_\varepsilon^n=v_\varepsilon^n((u_\varepsilon^n)^2)\in V_h$ solving:

$$(\delta_t v_\varepsilon^n,\bar v)^h+(\nabla v_\varepsilon^n,\nabla\bar v)+(v_\varepsilon^n,\bar v)^h=((u_\varepsilon^n)^2,\bar v),\ \ \forall\bar v\in V_h. \tag{47}$$

The well-posedness of problem (46) can be proved proceeding as Theorem 4.6 and Lemma 4.7 of [11]; while Lax-Milgram theorem implies the existence and uniqueness of solution for (47). The details are omitted.

4.2. Mass-conservation and energy-stability

In this subsection, we are going to present some properties of the scheme $\mathbf{US}_\varepsilon$; we highlight that these properties can be obtained independently of the choice of $\Lambda_\varepsilon(u_\varepsilon^n)$ approximating u_ε^n.

Since $\bar u=1\in U_h$ and $\bar v=1\in V_h$, then the scheme $\mathbf{US}_\varepsilon$ is conservative in u_ε^n, that is,

$$(u_\varepsilon^n,1)=(u_\varepsilon^n,1)^h=(u_\varepsilon^{n-1},1)^h=\cdots=(u_h^0,1)^h=(u_h^0,1)=(Q^hu_0,1)=(u_0,1)=m_0|\Omega|, \tag{48}$$

and also has the behaviour for $\int_\Omega v_\varepsilon^n$ given in (19) (with u_ε^n and v_ε^n instead of u_h^n and v_h^n respectively).

Definition 4.4. A numerical scheme with solution $(u_\varepsilon^n,\boldsymbol{\sigma}_\varepsilon^n)$ is called energy-stable if the energy

$$\widetilde{\mathcal{E}}(u,\boldsymbol{\sigma})=\frac{1}{2}\|u\|_0^2+\frac{1}{4}\|\boldsymbol{\sigma}\|_0^2 \tag{49}$$

is time decreasing, that is,

$$\widetilde{\mathcal{E}}(u_\varepsilon^n,\boldsymbol{\sigma}_\varepsilon^n)\le\widetilde{\mathcal{E}}(u_\varepsilon^{n-1},\boldsymbol{\sigma}_\varepsilon^{n-1}),\ \ \forall n\ge 1. \tag{50}$$

Now, in the following result, the energy stability property for the scheme $\mathbf{US}_\varepsilon$ with respect to the modified energy $\widetilde{\mathcal{E}}(u,\boldsymbol{\sigma})$ given in Definition 4.4 is stablished.

Theorem 4.5. (Unconditional stability) *The scheme $\mathbf{US}_\varepsilon$ is unconditionally energy stable with respect to the modified energy $\widetilde{\mathcal{E}}(u,\boldsymbol{\sigma})$ given in (49). In fact, if $(u_\varepsilon^n,\boldsymbol{\sigma}_\varepsilon^n)$ is a solution of $\mathbf{US}_\varepsilon$, then the following discrete energy law holds*

$$\delta_t\widetilde{\mathcal{E}}(\hat u_\varepsilon^n,\boldsymbol{\sigma}_\varepsilon^n)+\frac{k}{2}\|\delta_t\hat u_\varepsilon^n\|_0^2+\frac{k}{4}\|\delta_t\boldsymbol{\sigma}_\varepsilon^n\|_0^2+\|\hat u_\varepsilon^n\|_1^2+\frac{1}{2}\|\boldsymbol{\sigma}_\varepsilon^n\|_1^2\le 0. \tag{51}$$

Proof. Testing $(46)_1$ by $\bar u=\hat u_\varepsilon^n$, $(46)_2$ by $\bar{\boldsymbol{\sigma}}=\frac{1}{2}\boldsymbol{\sigma}_\varepsilon^n$ and adding the resulting expressions, the terms $(\Lambda_\varepsilon(u_\varepsilon^n)\nabla\hat u_\varepsilon^n,\boldsymbol{\sigma}_\varepsilon^n)$ cancel, and taking into account Remark 4.2, (51) is obtained. □

From (51), multiplying by k and summing, one can deduce the following global energy law:

Corollary 4.6. (Global energy law) *Assume that $(u_0,v_0)\in L^2(\Omega)\times H^1(\Omega)$. Let $(u_\varepsilon^n,\boldsymbol{\sigma}_\varepsilon^n)$ be any solution of scheme $\mathbf{US}_\varepsilon$. Then, the following estimate holds*

$$\|(\hat u_\varepsilon^n,\boldsymbol{\sigma}_\varepsilon^n)\|_0^2+k\sum_{m=1}^n\|(\hat u_\varepsilon^m,\boldsymbol{\sigma}_\varepsilon^m)\|_1^2\le C_0,\quad\forall n\ge 1.$$

4.3. Large-time behaviour of scheme $\mathbf{US}_\varepsilon$

In this part, exponential bounds for any solution $(u_h^n, \boldsymbol{\sigma}_h^n)$ of the scheme $\mathbf{US}_\varepsilon$ in weak norms are proved. The decay estimates obtained (see (52) and (53) below) can be seen as a discrete version of (12) and (16).

Theorem 4.7. *Let $(u_\varepsilon^n, \boldsymbol{\sigma}_\varepsilon^n)$ be any solution of the scheme $\mathbf{US}_\varepsilon$. Then, the following estimate holds*

$$\|(\hat{u}_\varepsilon^n, \boldsymbol{\sigma}_\varepsilon^n)\|_0^2 \le C_0 e^{-\frac{2K_p}{1+2K_p k}kn}, \quad \forall n \ge 0, \tag{52}$$

where the constant $K_p > 0$ was defined in Subsection 2.2.

Proof. Taking $\bar{u}_h = \hat{u}_\varepsilon^n$ in $(46)_1$, $\bar{\boldsymbol{\sigma}}_h = \frac{1}{2}\boldsymbol{\sigma}_\varepsilon^n$ in $(46)_2$ and using (48) as well as Remark 4.2, one obtains

$$\delta_t\Big(\frac{1}{2}\|\hat{u}_\varepsilon^n\|_0^2 + \frac{1}{4}\|\boldsymbol{\sigma}_\varepsilon^n\|_0^2\Big) + \frac{k}{2}\|\delta_t\hat{u}_\varepsilon^n\|_0^2 + \frac{k}{4}\|\delta_t\boldsymbol{\sigma}_\varepsilon^n\|_0^2 + \|\hat{u}_\varepsilon^n\|_1^2 + \frac{1}{2}\|\boldsymbol{\sigma}_\varepsilon^n\|_1^2 = 0.$$

Then, proceeding as in (35) and (41), one arrives at (52). □

Corollary 4.8. *Let $v_\varepsilon^n = v_\varepsilon^n((u_\varepsilon^n)^2)$ be a solution of (47). Then, it holds*

$$\|\hat{v}_\varepsilon^n\|_0^2 \le \begin{cases} Ce^{-\frac{1}{1+k}kn} & \text{if } 2K_p > 1, \\ C(kn)e^{-\frac{1}{1+k}kn} & \text{if } 2K_p = 1, \\ Ce^{-\frac{2K_p}{1+2K_p k}kn} & \text{if } 2K_p < 1, \end{cases} \tag{53}$$

where the constant $K_p > 0$ was defined in Subsection 2.2.

Proof. The proof follows as in Theorem 3.6; using, in this case, Remark 4.2. □

4.4. Positivity of v_ε^n and approximated positivity of u_ε^n

Unlike the scheme **UV** in which it is not clear how to prove positivity (neither exact nor approximate) for the discrete variables; for the scheme $\mathbf{US}_\varepsilon$ we will deduce exact positivity for v_h^n and approximated positivity for u_h^n. First, the positivity of the discrete chemical signal v_ε^n will be proved. For this, it will be essential that the interior angles of the triangles or tetrahedra are less than or equal to $\pi/2$. Since we impose the right angled constraint (**H**), then this property holds.

Lemma 4.9. (Positivity of v_ε^n) *Given $u_\varepsilon^n \in U_h$ and $v_\varepsilon^{n-1} \in V_h$, the unique $v_\varepsilon^n \in V_h$ solution of (47) satisfies $v_\varepsilon^n \ge 0$.*

Proof. We define $v_{\varepsilon-}^n := \min\{v_\varepsilon^n, 0\}$ and $v_{\varepsilon+}^n := \max\{v_\varepsilon^n, 0\}$. Then, testing (47) by $\bar{v} = \Pi^h(v_{\varepsilon-}^n) \in V_h$, and taking into account that $(\nabla\Pi^h(v_{\varepsilon+}^n), \nabla\Pi^h(v_{\varepsilon-}^n)) \ge 0$ (owing to the interior angles of the triangles or tetrahedra are less than or equal to $\pi/2$), and using that $(\Pi^h(v))^2 \le \Pi^h(v^2)$ for all $v \in C(\overline{\Omega})$, one has

$$\Big(\frac{1}{k} + 1\Big)\|\Pi^h(v_{\varepsilon-}^n)\|_0^2 + \|\nabla\Pi^h(v_{\varepsilon-}^n)\|_0^2 \le 0,$$

and the proof is concluded. □

Notice that the above properties were proved independently of the choice of $\Lambda_\varepsilon(u_\varepsilon^n)$ approximating u_ε^n. Now, in order to obtain approximated positivity for the discrete cell density u_ε^n, we need to consider $\Lambda_\varepsilon(u_\varepsilon^n)$ satisfying (44) and (45). The main idea in the proof is to get the following bound

$$(F_\varepsilon(u_\varepsilon^n), 1)^h \le C \tag{54}$$

which, following the ideas of Corollary 3.9 and Remark 3.12 of [11], implies the estimate (55) below, from which one can deduce that $u_{\varepsilon-}^n \to 0$ as $\varepsilon \to 0$ in the $L^2(\Omega)$-norm.

Theorem 4.10. (Approximated positivity of u_ε^n) *Let $(u_\varepsilon^n, \boldsymbol{\sigma}_\varepsilon^n)$ any solution of the scheme $\mathbf{US}_\varepsilon$. If $\varepsilon \in (0, e^{-2})$, the following estimate holds*

$$\max_{n\ge 0}\|\Pi^h(u_{\varepsilon-}^n)\|_0^2 \le C_0\varepsilon, \tag{55}$$

where the constant C_0 depends on the data (Ω, u_0, v_0), but is independent of k, h, n and ε.

Proof. Testing $(46)_1$ by $\bar{u} = \Pi^h(F'_\varepsilon(u^n_\varepsilon))$ and taking into account that $\Lambda_\varepsilon(u^n_\varepsilon)$ is symmetric as well as (44) (which implies that $\nabla\Pi^h(F'_\varepsilon(u^n_\varepsilon)) = \Lambda_\varepsilon^{-1}(u^n_\varepsilon)\nabla u^n_\varepsilon$), one obtains

$$(\delta_t u^n_\varepsilon, \Pi^h(F'_\varepsilon(u^n_\varepsilon)))^h + \int_\Omega (\nabla u^n_\varepsilon)^T \cdot \Lambda_\varepsilon^{-1}(u^n_\varepsilon) \cdot \nabla u^n_\varepsilon d\boldsymbol{x} = -\int_\Omega \boldsymbol{\sigma}^n_\varepsilon \cdot \nabla u^n_\varepsilon d\boldsymbol{x}. \tag{56}$$

By using the Taylor formula and taking into account that Π^h is linear and $F''_\varepsilon(s) \geq \varepsilon$ for all $s \in \mathbb{R}$, one has (following [11, Theorem 3.8])

$$(\delta_t u^n_\varepsilon, \Pi^h(F'_\varepsilon(u^n_\varepsilon)))^h \geq \delta_t(F_\varepsilon(u^n_\varepsilon), 1)^h + \varepsilon\frac{k}{2}|\delta_t u^n_\varepsilon|^2_h,$$

which, together with (45), (56) and Remark 4.2, imply that

$$\delta_t(F_\varepsilon(u^n_\varepsilon), 1)^h + \varepsilon\frac{k}{2}\|\delta_t u^n_\varepsilon\|^2_0 + \varepsilon\|\nabla u^n_\varepsilon\|^2_0 \leq \frac{1}{2}\|\nabla u^n_\varepsilon\|^2_0 + \frac{1}{2}\|\boldsymbol{\sigma}^n_\varepsilon\|^2_0. \tag{57}$$

Then, multiplying (57) by k, adding for $n = 1, \cdots, m$ and using Corollary 4.6, one arrives at

$$(F_\varepsilon(u^m_\varepsilon), 1)^h \leq (F_\varepsilon(u^0_h), 1)^h + k\sum_{n=1}^m \left(\frac{1}{2}\|\nabla u^n_\varepsilon\|^2_0 + \frac{1}{2}\|\boldsymbol{\sigma}^n_\varepsilon\|^2_0\right) \leq C_0,$$

where $C_0 > 0$ is a constant depending on the data (Ω, u_0, v_0), but independent of k, h, n and ε. Thus, (54) is obtained. Therefore, if $\varepsilon \in (0, e^{-2})$, from $(43)_2$ and following the proof of Corollary 3.9 and Remark 3.12 of [11], (55) is deduced. □

5. Numerical simulations

In this section we will show several numerical simulations that we have carried out using the two schemes studied in the paper, comparing them with the following ones, the scheme **US** studied in [13], the classical backward Euler scheme associated to (1) with $(\mathbb{P}_1, \mathbb{P}_1)$-continuous approximation for (u^n_h, v^n_h) (called Scheme **BE** from now on), and a linear characteristic method analogous to one considered in [29] for the Keller-Segel system (called Scheme **CH** from now on), in which we have changed the chemo-attraction term by a chemo-repulsion term and the linear production term by a quadratic production. We are considering $(\mathbb{P}_1, \mathbb{P}_2)$-continuous approximation for (u^n_h, v^n_h). Moreover, we have chosen the domain $\Omega = [0, 2]^2$ using a structured mesh, and all the simulations are carried out using **FreeFem++** software. We use Newton's method to approach the nonlinear schemes **US**, **UV** and **BE**; while for the scheme $\mathbf{US}_\varepsilon$, we use the following Picard method:

- Picard method to approach a solution $(u^n_\varepsilon, \boldsymbol{\sigma}^n_\varepsilon)$ of the scheme $\mathbf{US}_\varepsilon$:
  Initialization $(l = 0)$**:** Set $(u^0_\varepsilon, \boldsymbol{\sigma}^0_\varepsilon) = (u^{n-1}_\varepsilon, \boldsymbol{\sigma}^{n-1}_\varepsilon) \in U_h \times \boldsymbol{\Sigma}_h$.
  Algorithm: Given $(u^l_\varepsilon, \boldsymbol{\sigma}^l_\varepsilon) \in U_h \times \boldsymbol{\Sigma}_h$, compute $(u^{l+1}_\varepsilon, \boldsymbol{\sigma}^{l+1}_\varepsilon) \in U_h \times \boldsymbol{\Sigma}_h$ such that

$$\begin{cases} \frac{1}{k}(u^{l+1}_\varepsilon, \bar{u})^h + (\nabla u^{l+1}_\varepsilon, \nabla\bar{u}) = \frac{1}{k}(u^{n-1}_\varepsilon, \bar{u})^h - (\Lambda_\varepsilon(u^l_\varepsilon)\boldsymbol{\sigma}^l_\varepsilon, \nabla\bar{u}), \quad \forall \bar{u} \in U_h, \\ \frac{1}{k}(\boldsymbol{\sigma}^{l+1}_\varepsilon, \bar{\boldsymbol{\sigma}}) + (B\boldsymbol{\sigma}^{l+1}_\varepsilon, \bar{\boldsymbol{\sigma}}) = \frac{1}{k}(\boldsymbol{\sigma}^{n-1}_\varepsilon, \bar{\boldsymbol{\sigma}}) + (\Lambda_\varepsilon(u^{l+1}_\varepsilon)\nabla u^{l+1}_\varepsilon, \bar{\boldsymbol{\sigma}}), \quad \forall \bar{\boldsymbol{\sigma}} \in \Sigma_h, \end{cases}$$

  until the stopping criterion $\max\left\{\dfrac{\|u^{l+1} - u^l\|_0}{\|u^l\|_0}, \dfrac{\|\boldsymbol{\sigma}^{l+1} - \boldsymbol{\sigma}^l\|_0}{\|\boldsymbol{\sigma}^l\|_0}\right\} \leq tol.$

In all the cases, we consider $tol = 10^{-4}$.

5.1. Positivity

The aim of this subsection is to compare the fully discrete schemes **UV**, **US** and $\mathbf{US}_\varepsilon$ in terms of positivity. Theoretically, for all schemes, the positivity of the variable u^n_h is not clear. However, for the scheme $\mathbf{US}_\varepsilon$, it was proved that $\Pi^h(u^n_{\varepsilon-}) \to 0$ in $L^2(\Omega)$ as $\varepsilon \to 0$ (see Theorem 4.10). For this reason, in Fig. 2 we compare the positivity of the variable u^n in the schemes, taking the spatial parameter $h = 1/20$, a small time step $k = 10^{-5}$ (in order to see the differences in the spatial approximations), and the initial conditions (see Fig. 1):

$$u_0 = -10xy(2-x)(2-y)exp(-10(y-1)^2 - 10(x-1)^2) + 10.0001$$

and

$$v_0 = 100xy(2-x)(2-y)exp(-30(y-1)^2 - 30(x-1)^2) + 0.0001.$$

Note that $u_0, v_0 > 0$ in Ω, $\min(u_0) = u_0(1,1) = 0.0001$ and $\max(v_0) = v_0(1,1) = 100.0001$. We obtain that (see Fig. 2):

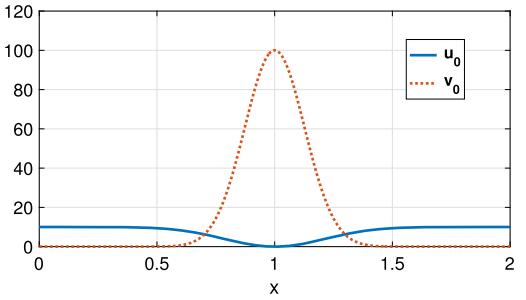

Fig. 1. Cross section at $y = 1$ of the initial cell density u_0 and chemical concentration v_0.

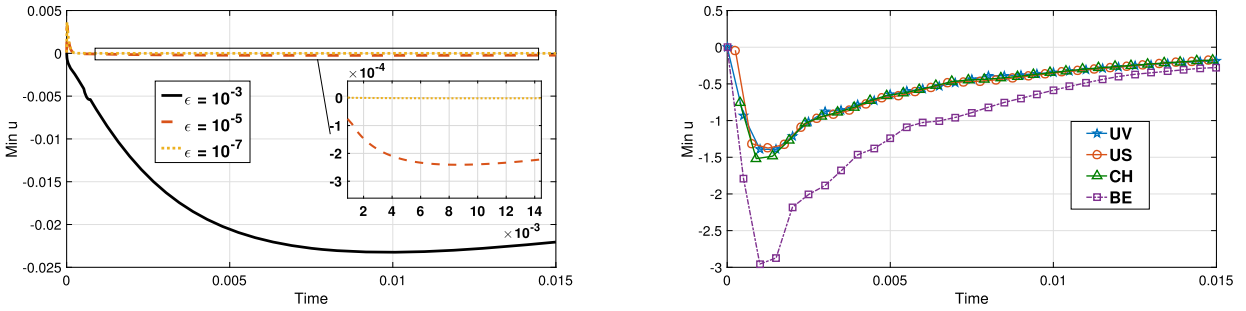

(a) Scheme $\mathbf{US}_\varepsilon$ (b) Schemes **UV**, **US**, **CH** and **BE**

Fig. 2. Minimum values of u_h^n.

1. In all schemes, the discrete cell density u_h^n takes negative values for some $\boldsymbol{x} \in \Omega$ in some times $t_n > 0$.
2. In the scheme $\mathbf{US}_\varepsilon$, the negative values of u_ε^n are closer to 0 as $\varepsilon \to 0$.
3. The scheme $\mathbf{US}_\varepsilon$ evidence "better positivity" than the schemes **UV**, **US**, **CH** and **BE** because the "greater" negative values for $\mathbf{US}_\varepsilon$ are of order 10^{-2}, while the another schemes reach values greater than -1, being the scheme **BE** the one that reaches the largest negative values.

5.2. ε-approximated positivity vs spurious oscillations

In this subsection, we present some numerical experiments relating the negativity of the discrete cell density observed in Subsection 5.1 with the spurious oscillations that could appear. With this aim, we consider $k = 10^{-5}$, $h = \frac{1}{25}$, $\varepsilon = 10^{-6}$ (for the scheme $\mathbf{US}_\varepsilon$) and the following initial conditions:

$$u_0 = 5cos(2\pi x)cos(2\pi y) + 5.0001 \text{ and } v_0 = -170cos(2\pi x)cos(2\pi y)) + 170.0001$$

in which, the places with the highest chemical concentration have lower cell density, in order to force to the cell density to be very close to zero. Note that $u_0, v_0 > 0$ in Ω, $\min(u_0) = u_0(1,1) = 0.0001$ and $\max(v_0) = v_0(1,1) = 170.0001$.

We observe that, in the case of the schemes **UV**, **US**, **CH** and **BE** some spuriuos oscillations appear when the discrete cell density takes negative values (which makes simulations unreliable in this "extreme" case); while, in the case of the scheme $\mathbf{US}_\varepsilon$, the ε-approximated positivity favours the non-appearance of spurious oscillations (see Figs. 3, 4).

5.3. Energy-stability

Previously, it was proved that the scheme **UV** is unconditionally energy-stable with respect to the energy $\mathcal{E}(u, v)$ given in (10) (in the primitive variables (u, v)), the schemes **US** and $\mathbf{US}_\varepsilon$ are unconditionally energy-stable with respect to the modified energy $\widetilde{\mathcal{E}}(u, \boldsymbol{\sigma})$ given in (49), and for the schemes **CH** and **BE** it is not clear how to obtain an energy stability property. In this section, we compare numerically the energy stability of the schemes with respect to the "exact" energy $\mathcal{E}(u, v)$ which comes from the continuous problem, and we also study the behaviour of the corresponding discrete residual of the energy law (9):

$$RE^n := \delta_t \mathcal{E}(u_h^n, v_h^n) + \|\nabla u_h^n\|_0^2 + \frac{1}{2}\|(A_h - I)v_h^n\|_0^2 + \frac{1}{2}\|\nabla v_h^n\|_0^2.$$

With this aim, we consider the parameters $k = 10^{-6}$ (in order to minimize the influence of the numerical dissipation terms $\frac{k}{2}\|\delta_t u_h^n\|_0^2$ and $\frac{k}{4}\|\delta_t \nabla v_h^n\|_0^2$ (or $\frac{k}{4}\|\delta_t \boldsymbol{\sigma}_h^n\|_0^2$) appearing in (23) and (51)), $h = \frac{1}{25}$ and the initial conditions

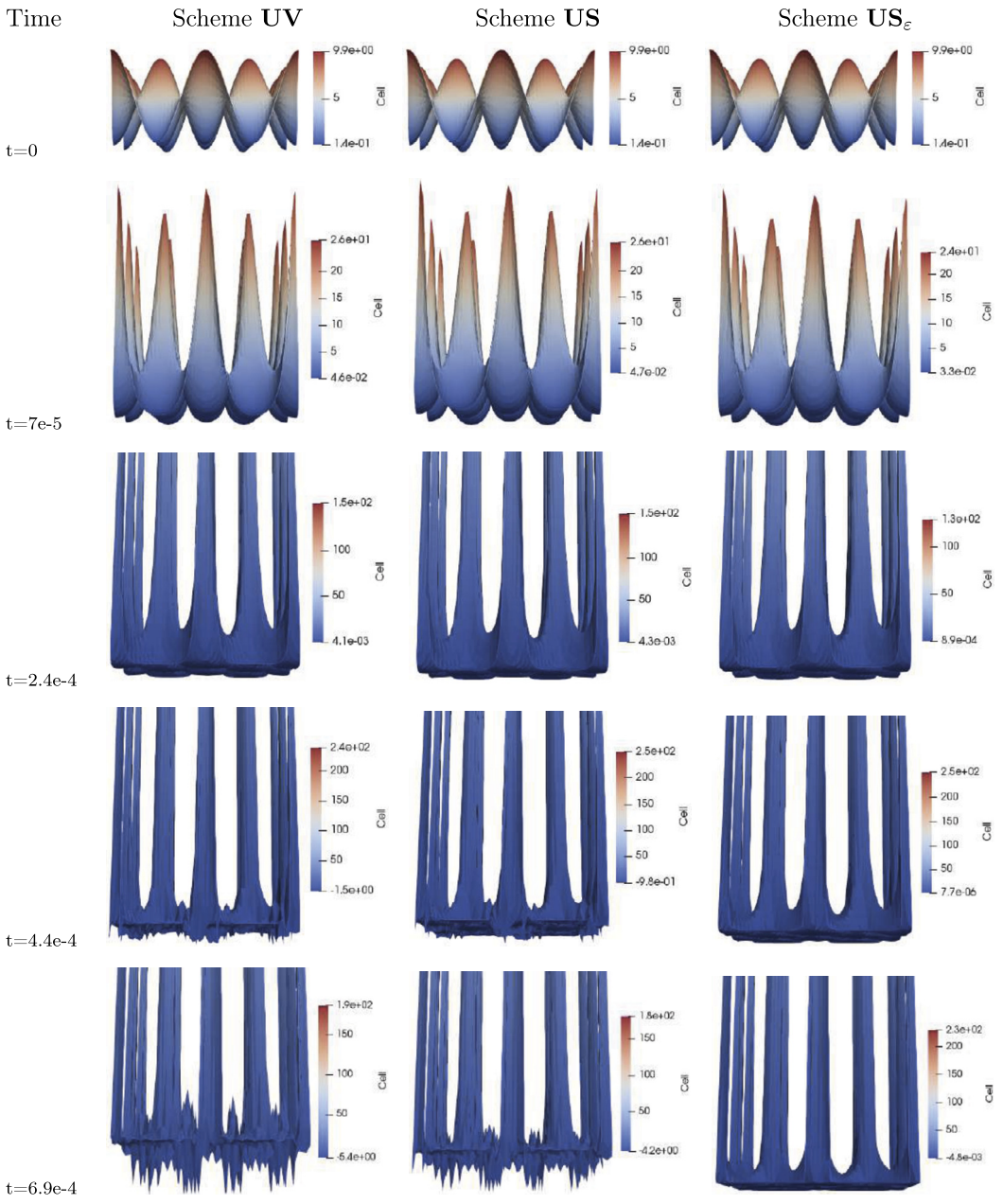

Fig. 3. Positivity vs spurious oscillations of the discrete cell density for the schemes **UV**, **US** and **US**$_\varepsilon$.

$$u_0 = -10xy(2-x)(2-y)exp(-10(y-1)^2 - 10(x-1)^2) + 10.0001$$

and

$$v_0 = 20xy(2-x)(2-y)exp(-30(y-1)^2 - 30(x-1)^2) + 0.0001,$$

obtaining that:

(a) All schemes satisfy the energy decreasing in time property for the energy $\mathcal{E}(u, v)$, that is, $\mathcal{E}(u_h^n, v_h^n) \leq \mathcal{E}(u_h^{n-1}, v_h^{n-1})$ for all n, see Fig. 5(a).

(b) The scheme **UV** satisfies the discrete energy law $RE^n \leq 0$ for all $n \geq 1$; while the schemes **US**$_\varepsilon$, **US**, **BE** and **CH** evidence positive values for RE^n for some $n \geq 1$, being the scheme **CH** that reaches the largest positive values (see Fig. 5(b)-(c)).

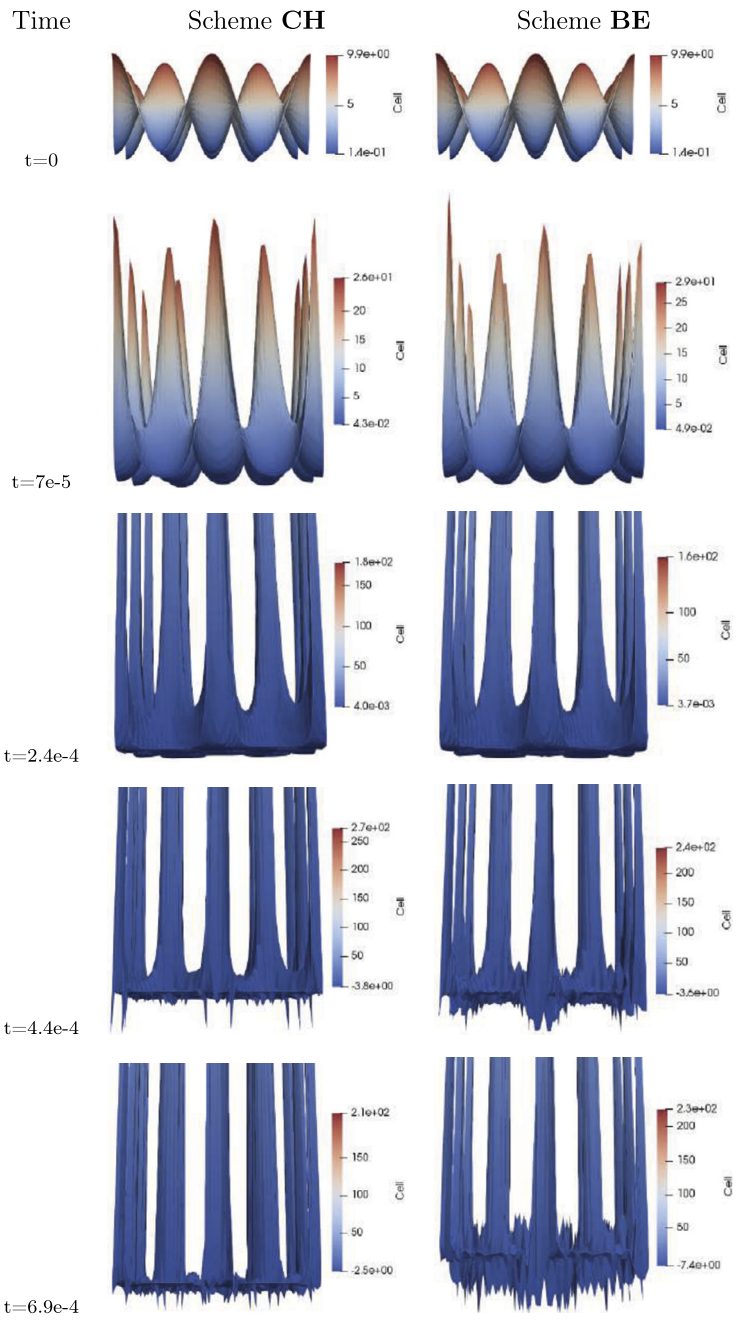

Fig. 4. Positivity vs spurious oscillations of the discrete cell density for the schemes **CH** and **BE**.

5.4. Asymptotic behaviour

In this subsection, we present some numerical experiments in order to illustrate the large-time behaviour of approximated solutions computed by using the schemes **UV**, **US** and $\mathbf{US}_\varepsilon$ in two different situations. In the first test, we consider the initial conditions such that the places with the highest chemical concentration have lower cell density; while in the second test, the places with the highest initial chemical concentration have the highest initial cell density. In both situations, we consider $k = 10^{-3}$ and $h = \frac{1}{25}$. Moreover, for the scheme $\mathbf{US}_\varepsilon$, we consider $\varepsilon = 10^{-5}$.

- Test 1: We choose the initial conditions (see Fig. 6):

$$u_0^1 = 5cos(2\pi x)cos(2\pi y) + 5.0001 \text{ and } v_0^1 = -15cos(2\pi x)cos(2\pi y) + 24.$$

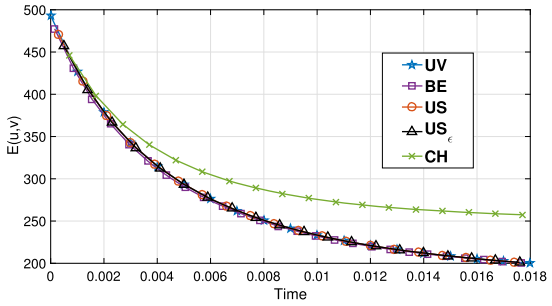

(a) Energy $\mathcal{E}(u_h^n, v_h^n)$

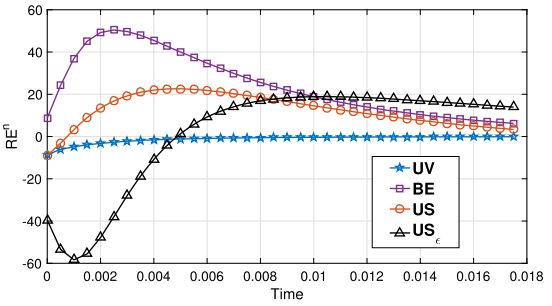

(b) Discrete residual RE^n of the schemes **UV**, **BE**, $\mathbf{US}_\varepsilon$ and **US**

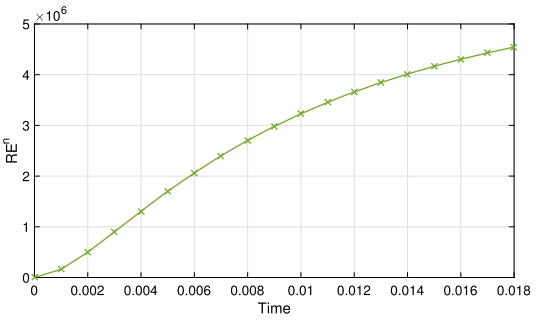

(c) Discrete residual RE^n of the scheme **CH**

Fig. 5. Energy-stability of the schemes.

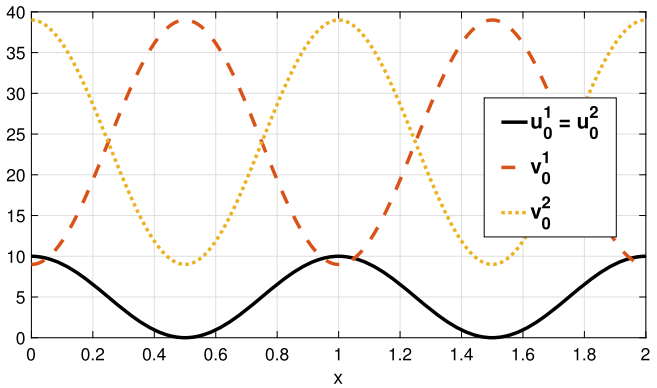

Fig. 6. Cross section at $y = 1$ of the initial cell densities $u_0^1 = u_0^2$ and chemical concentrations v_0^1, v_0^2.

- Test 2: We choose the initial conditions:

$$u_0^2 = u_0^1 \text{ and } v_0^2 = 15cos(2\pi x)cos(2\pi y) + 24.$$

In both cases, we observe that $\|(u_h^n - m_0, \nabla v_h^n)\|_0^2$ decreases to 0 faster than $\|v_h^n - (m_0)^2\|_0^2$. In Figs. 7-8, on which the ordinate axis is on a logarithmic scale, we observe an exponential decay (at least) of (u_h^n, v_h^n) to $(m_0, (m_0)^2)$. These facts are in agreement with the theoretical results proved in this paper.

6. Conclusions

In this paper, we study two fully discrete FE schemes for a repulsive chemotaxis model with quadratic signal production, called **UV** (the FE backward Euler in variables (u, v)) and $\mathbf{US}_\varepsilon$ (obtained by mixing the scheme **US** proposed in [13] with a regularization technique). For these numerical schemes we obtain better properties than those proved for the scheme **US** in

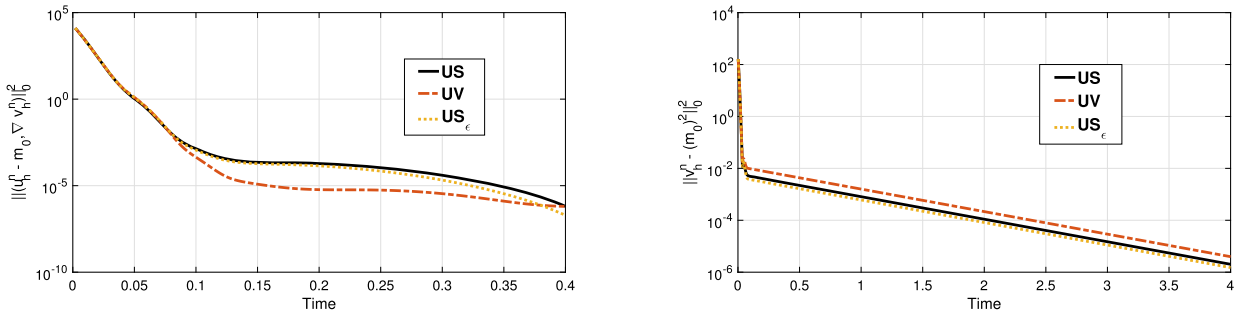

Fig. 7. Evolution of $\|(u_h^n - m_0, \nabla v_h^n)\|_0^2$ and $\|v_h^n - (m_0)^2\|_0^2$ in test 1.

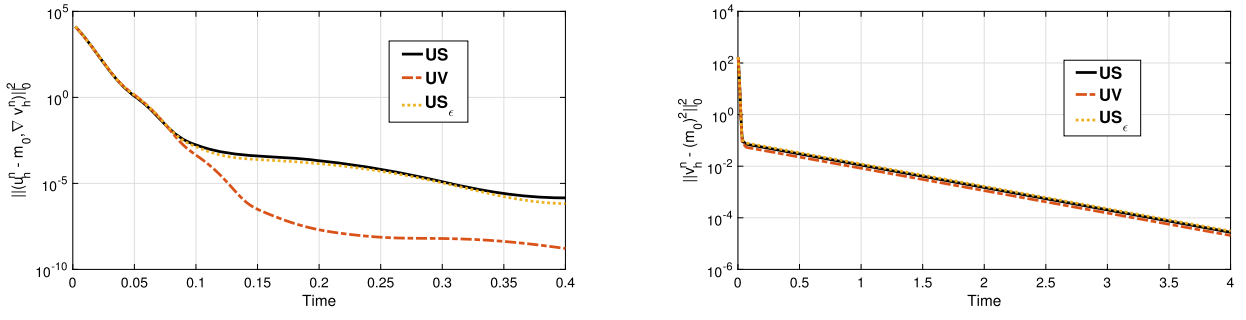

Fig. 8. Evolution of $\|(u_h^n - m_0, \nabla v_h^n)\|_0^2$ and $\|v_h^n - (m_0)^2\|_0^2$ in test 2.

[13]. Specifically, the comparison between the numerical schemes **UV** and **US**$_\varepsilon$, and the scheme **US**, allows us to conclude that, from the theoretical point of view:

1. By imposing the "compatibility" condition $(\mathbb{P}_m, \mathbb{P}_{2m})$-continuous FE (with $m \geq 1$) for (u, v), the scheme **UV** is energy-stable (in the primitive variables (u, v)). In the case of the schemes **US** and **US**$_\varepsilon$, it can be obtained energy-stability but with respect to a modified energy written in terms of $(u, \boldsymbol{\sigma})$.
2. As a consequence of item 1, the exponential convergence of the scheme **UV** to the constant states m_0 and $(m_0)^2$ (when the time goes to infinity) can be proved in weak norms for u and strong norms for v (equal than the continuous case); while in the schemes **US** and **US**$_\varepsilon$, it can be also proved exponential convergence towards m_0 and $(m_0)^2$, but only in weak norms for u and v.
3. Approximated positivity for the discrete solutions is proved for the scheme **US**$_\varepsilon$, but it is not clear how to prove neither positivity nor approximated positivity for the schemes **US** and **UV**.

From the numerical point of view, comparing these schemes with a linear characteristic method analogous to one considered in [29] for the Keller-Segel system (Scheme **CH**) and the classical backward Euler scheme associated to (1) with $(\mathbb{P}_1, \mathbb{P}_1)$-continuous approximation for (u_h^n, v_h^n) (Scheme **BE**), we have obtained that:

1. The scheme **US**$_\varepsilon$ shows "better positivity" than the schemes **UV**, **US**, **CH** and **BE**. Moreover, for the scheme **US**$_\varepsilon$ it was observed numerically that $\min_{\overline{\Omega}\times[0,T]} u_\varepsilon^n \to 0$ as $\varepsilon \to 0$.
2. In some cases, for example when negative values are obtained for u_h, some spurious oscillations are observed in the schemes **UV**, **US**, **CH** and **BE**; while in the scheme **US**$_\varepsilon$, the approximated positivity of u_h favours the non-appearance of spurious oscillations.
3. All schemes have decreasing in time energy $\mathcal{E}(u, v)$.
4. It is observed an exponential decay (at least) of (u_h^n, v_h^n) in weak-strong norm to $(m_0, (m_0)^2)$.

Acknowledgements

The authors have been partially supported by MINECO grant MTM2015-69875-P (Ministerio de Economía y Competitividad, Spain) with the participation of FEDER. The first and second authors have also been supported by Grant PGC2018-098308-B-I00 by MCIN/AEI/ 10.13039/501100011033 and by ERDF A way of making Europe; and the third author has also been supported by Vicerrectoría de Investigación y Extensión of Universidad Industrial de Santander, Colombia, project

“Análisis teórico de problemas difereciales con difusión cruzada: aplicaciones al estudio de dinámicas poblacionales”, code C-2020-06.

References

[1] C. Amrouche, N.E.H. Seloula, L^p-theory for vector potentials and Sobolev's inequalities for vector fields: application to the Stokes equations with pressure boundary conditions, Math. Models Methods Appl. Sci. 23 (1) (2013) 37–92.
[2] J.W. Barrett, J.F. Blowey, Finite element approximation of a nonlinear cross-diffusion population model, Numer. Math. 98 (2) (2004) 195–221.
[3] R. Becker, X. Feng, A. Prohl, Finite element approximations of the Ericksen-Leslie model for nematic liquid crystal flow, SIAM J. Numer. Anal. 46 (2008) 1704–1731.
[4] N. Bellomo, M. Winkler, Finite-time blow-up in a degenerate chemotaxis system with flux limitation, Trans. Am. Math. Soc. Ser. B 4 (2017) 31–67.
[5] M. Bessemoulin-Chatard, A. Jüngel, A finite volume scheme for a Keller-Segel model with additional cross-diffusion, IMA J. Numer. Anal. 34 (1) (2014) 96–122.
[6] G. Chamoun, M. Saad, R. Talhouk, Numerical analysis of a chemotaxis-swimming bacteria model on a general triangular mesh, Appl. Numer. Math. 127 (2018) 324–348.
[7] X. Chen, F. Hu, J. Zhang, J. Shen, Global existence and blow-up for a chemotaxis system, Math. Model. Anal. 22 (2) (2017) 237–251.
[8] T. Cieslak, P. Laurencot, C. Morales-Rodrigo, Global existence and convergence to steady states in a chemorepulsion system, in: Parabolic and Navier-Stokes Equations. Part 1, in: Banach Center Publ., vol. 81, Polish Acad. Sci. Inst. Math., Warsaw, 2008, pp. 105–117.
[9] P. De Leenheer, J. Gopalakrishnan, E. Zuhr, Nonnegativity of exact and numerical solutions of some chemotactic models, Comput. Math. Appl. 66 (3) (2013) 356–375.
[10] F. Guillén-González, M. Samsidy, Stability and convergence at infinite time of several fully discrete schemes for a Ginzburg-Landau model for nematic liquid crystal flows, Discrete Contin. Dyn. Syst. 32 (12) (2012) 4229–4246.
[11] F. Guillén-González, M.A. Rodríguez-Bellido, D.A. Rueda-Gómez, Unconditionally energy stable fully discrete schemes for a chemo-repulsion model, Math. Comput. 88 (319) (2019) 2069–2099.
[12] F. Guillén-González, M.A. Rodríguez-Bellido, D.A. Rueda-Gómez, Study of a chemo-repulsion model with quadratic production. Part I: analysis of the continuous problem and time-discrete numerical schemes, Comput. Math. Appl. 80 (2020) 692–713.
[13] F. Guillén-González, M.A. Rodríguez-Bellido, D.A. Rueda-Gómez, Study of a chemo-repulsion model with quadratic production. Part II: analysis of an unconditionally energy-stable fully discrete scheme, Comput. Math. Appl. 80 (2020) 636–652.
[14] T. Hillen, K.J. Painter, A user's guide to PDE models for chemotaxis, J. Math. Biol. 58 (1–2) (2009) 183–217.
[15] S. Hittmeir, A. Jüngel, Cross diffusion preventing blow-up in the two-dimensional Keller-Segel model, SIAM J. Math. Anal. 43 (2) (2011) 997–1022.
[16] D. Horstmann, From 1970 until present: the Keller-Segel model in chemotaxis and its consequences. I, Jahresber. Dtsch. Math.-Ver. 105 (3) (2003) 103–165.
[17] E.F. Keller, L.A. Segel, Initiation of slime mold aggregation viewed as an instability, J. Theor. Biol. 26 (1970) 399–415.
[18] E. Lankeit, J. Lankeit, On the global generalized solvability of a chemotaxis model with signal absorption and logistic growth terms, Nonlinearity 32 (5) (2019) 1569–1596.
[19] J. Lankeit, M. Winkler, A generalized solution concept for the Keller-Segel system with logarithmic sensitivity: global solvability for large nonradial data, Nonlinear Differ. Equ. Appl. 24 (4) (2017) 49.
[20] K. Lin, C. Mu, H. Zhong, A blow-up result for a quasilinear chemotaxis system with logistic source in higher dimensions, J. Math. Anal. Appl. 464 (1) (2018) 435–455.
[21] B. Merlet, M. Pierre, Convergence to equilibrium for the backward Euler scheme and applications, Commun. Pure Appl. Anal. 9 (2010) 685–702.
[22] J. Necas, Les Methodes Directes en Theorie des Equations Elliptiques, Editeurs Academia, Prague, 1967.
[23] K. Osaki, A. Yagi, Finite dimensional attractors for one-dimensional Keller-Segel equations, Funkc. Ekvacioj 44 (2001) 441–469.
[24] Y. Tao, M. Winkler, Boundedness vs. blow-up in a two-species chemotaxis system with two chemicals, Discrete Contin. Dyn. Syst., Ser. B 20 (9) (2015) 3165–3183.
[25] G. Viglialoro, Explicit lower bound of blow-up time for an attraction-repulsion chemotaxis system, J. Math. Anal. Appl. 479 (1) (2019) 1069–1077.
[26] Y. Wang, M. Winkler, Z. Xiang, The small-convection limit in a two-dimensional chemotaxis-Navier-Stokes system, Math. Z. 289 (1–2) (2018) 71–108.
[27] M. Winkler, Finite-time blow-up in low-dimensional Keller-Segel systems with logistic-type superlinear degradation, Z. Angew. Math. Phys. 69 (2) (2018) 69.
[28] M. Winkler, Global existence and stabilization in a degenerate chemotaxis-Stokes system with mildly strong diffusion enhancement, J. Differ. Equ. 264 (10) (2018) 6109–6151.
[29] J. Zhang, J. Zhu, R. Zhang, Characteristic splitting mixed finite element analysis of Keller-Segel chemotaxis models, Appl. Math. Comput. 278 (2016) 33–44.
[30] J. Zhao, C. Mu, L. Wang, D. Zhou, Blow-up and bounded solutions in a two-species chemotaxis system in two dimensional domains, Acta Appl. Math. 153 (2018) 197–220.
[31] G. Zhou, N. Saito, Finite volume methods for a Keller-Segel system: discrete energy, error estimates and numerical blow-up analysis, Numer. Math. 135 (1) (2017) 265–311.